*Indian Journal of Fundamental and Applied Life Sciences ISSN: 2231– 6345 (Online)*
*An Open Access, Online International Journal Available at www.cibtech.org/sp.ed/jls/2014/03./jls.htm*
*2014 Vol. 4 (S3), pp. 154-167/Tariverdian and Farhoudi*
***Research Article***

# THE ALTERATION IN FLEXURAL ULTIMATE STRENGTH OF PLATE GIRDERS WITH DISTRIBUTED LAODDUE TO CRACKS OCCURRING IN THE FLANGE TO WEB WELD

***Hamoun Tariverdian and Farhad Farhoudi**
*Department of Civil Engineering, Sardroud Branch, Islamic Azad University, Sardroud, Iran*
**Author for Correspondence*

## ABSTRACT
Plate girders are seed as important structural members for covering large flexural spans, and are the result of the welding of two flanges to one web plate. To prevent the buckling of the web plate, vertical or longitudinal stiffeners are connected to it. Because of the importance of the flange-web weld in the structural behavior of plate girders and the possibility of occurrence of cracks, either during the welding or later, due to physical or environmental elements, this article studies the effect of cracks in the flange-web weld of the plate girders on their flexural ultimate capacity. Various analytical models were built and studied, using the limited element software LUSAS. All the AISC-LRFD Codes were observed in the designing of the models. And the connection of the flanges to the web were carried out with continuous welding. For the modelization of the plate girders, the four-sided, eight-node shell element was used, and they were analyzed in a nonlinear geometric and physical method. For more realistic results, a primary $10_{mm}$ imperfection was presumed in the middle of the web of the plate girder. The physical behavior of the materials was also presumed to be 4-linear non-elastic. These plate girders also used St40kis steel with yielding strength of 2750 $Kg/cm^2$. The imposed load on the upper flange was even, linear and distributed, and the supports of both sides of the girder were fixed and moving articulations. The results of the study showed that the occurrence of cracks in critical panels can reduce at most %18 of the flexural ultimate capacity in this type of plate girders.

***Keywords:*** *Plate Girder, Crack, Weld, Web, Flange, Flexural Strength*

## INTRODUCTION
With today`s advanced Technology, the use of huge structural systems in increasing service rendering and profiting has been unavoidable. Since such structures have large spans and often considerable imposed loads, one way for providing the required cross section is the use of plate girders.
Until the year 1981, plate girders were designed on the basis of the control of elastic buckling in the pieces made of plates so that the rules of designing plate girders were based on the theory of elasticity due to slight alterations. In other words, it was presumed that the standard system was likely to fall apart due to elastic instability or yielding (Akbari, 2006).
Bassler *et al.*, revealed that after the lateral deflections in the plate girders due to shearing buckling occur, a series of membrane tensile stresses are produces in the middle plane of the plate, which tend to return the plate to its steady state. In fact, it is because of the effect of these stresses that sudden buckling do not appear in plates as they do in columns and they show great load bearing capacity even after buckling. Therefore, the new codes of practice contain items which discuss the post buckling capacity. In the sense that if a plate girder has not been designed correctly and has vertical stiffeners, it will act as a truss after the buckling of the web, in which case the buckled web will act as the tensile diameters and the vertical stiffeners as compressive flanges of the truss (Tahooni, 2001).
The complicated behaviour of plate girders and the differing methods of their design have led to extensive researches of which one of the most important is the study of the impact of cracks of different parts of the plate girders on their bending and buckling behaviour. Cracks in plate girders are caused by fatigue, metal corrosion, deflective effects, abundance of tension and luck of attention to necessary standards in welding their parts. It must be noticed that the behaviour of the crack including its speed and direction of distribution and the age of fatigue depends on the quality of the weld, the residual tensions resulting from

welding and rolling of the steel plates, the surrounding area of the structure (from the point of view of moisture, corrosion and acidity of environment) and the type of loading of the structure. In recent years, many researches have been done on the causes of cracks their distribution the effect of environmental factors on the rate of their distribution and the assessment of fatigue life of engineering structures, especially in plate girders of bridges.

In 1960, numerous experiments were carried out in Japan and the US on slender plate girders with vertical or longitudinal stiffeners. In most of these experiments, panels of plate girders were influenced by shearing, bending or a combination of both. The results show that the type and location of fatigue cracks are related to the change in the direction of buckling of the web plate in the panel during the loading cycles known as web breathing. These studies revealed that the presence of primary imperfection in the web plate, the dimensional ratio of the plate girder ( $a/h$ ) and the ratio of its slenderness ( $h/t_w$ ) are the main factors of causing such cracks. In fact, it is possible to prevent cracks due to web breathing by using plates with very little primary imperfection while paying extra attention to the production, transport and assembly of plates used in construction of plate girders and limiting the dimensional and slenderness ratios. (Roberts and Davies, 2002)

In 1993, extensive studies by Fisher *et al.*, about the location of cracks caused shearing, bending or a combination of both revealed that most of the cracks resulting from welding of the flange to the web of the plate girder started from the toe of the fillet weld on the web and distributed through the thickness of the web. If the location of the cracks were at the beginning or the end of the web panel, the speed of the distribution of the cracks in the middle of the web panel would be higher, which in turn would result in destruction of the structure due to buckling of the compressive flange and web (Nicola Greco, 2000). Simultaneously, Corcetti carries out studies on four large plate girders and concluded that fatigue cracks started from the toe of the weld on the web of the plate girders (Corcetti, 2003)

In 2005, Experiments by Paik *et al.*, to determine the final capacity of cracked plates under axial, compressive and tensile loading showed that the existence of fatigue cracks reduced the final resistance of metal plates; and that the length of the crack and the thickness of the plate played an important role in this reduction. They also found out that if a crack occurs in a panel under pressure, it will close and then buckle, causing deformations and loading will be done locally and out of the plate. This study indicated that the increase in the thickness of the plates with cracks in the edges of the panels caused the increase of the strength-reduction factor: that is, the thicker the plate, the more effective the cracks in the reduction of the resistance capacity.

Figure 1 shows the results of the theses studies (Paik, *et al.*, 2005).

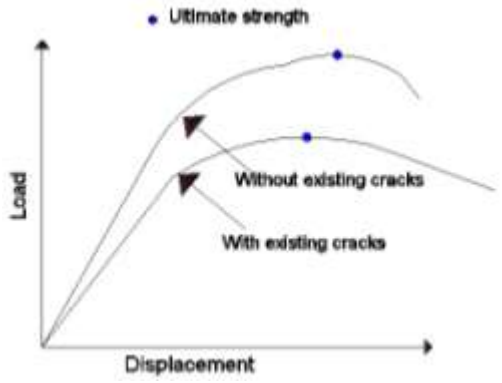


**Figure1: load-displacement graph in cracked and uncracked positions (Paik, *et al.*, 2005)**

With regards to previous studies, this article has tried to examine the changes in the final bending capacity of plate girders by developing cracks in the weld of the flange to the web of plate girders.

***Research Article***

***Modelization and Analysis of Samples***

In this research the limited element software LUSAS was used. This software (LUSAS) has very high limited element capacity which ranges from simple linear and static analysis with nonlinear time history.

First, a simple beam with loads and support conditions as illustrated in figure 2 is designed according to the LRFD codes of practice and the geometric specifications obtained from the LUSAS were modelized. (Figure 2)

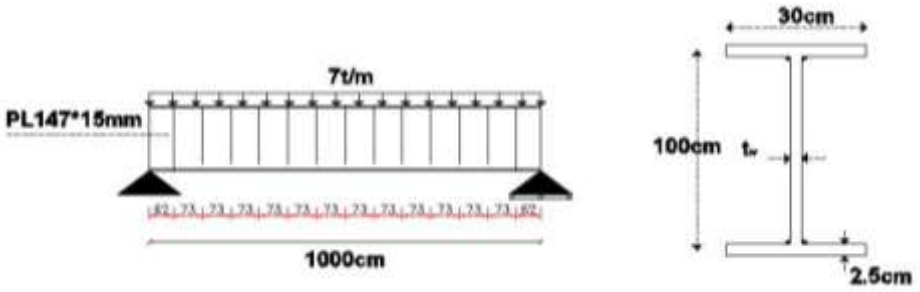


**Figure 2: The geometric specifications of the plate girder**

Since it is practically very difficult to achieve a structure without any primary imperfection and imperfections are usually found in the web plates of plate girders, a primary imperfection in the form of serious half wave was made in the direction of the length and height of the behaviour of the plate girders more practically and precisely and precisely and to bring the achieved results closer to the real results. The maximum amount of this imperfection was about 1/1000 of the length of the span (1 $_{cm}$) in the middle of the panel. To make the model of the web with a primary infection, equation 1, which is a sinus equation, was used.

$$X = \delta \times Sin(\frac{\pi y}{h}) Sin(\frac{\pi z}{a}) \quad (1)$$

In this equation, ( $a$ ) is the length of the panel, ( $h$ ) is the height of panel and ( $\delta$ ) is the maximum deflection (pitch) in the middle of the panel. ( $y$ ) is the vertical axis and ( $z$ ) is the longitudinal axis of the girder.

In should be mentioned that in the making process of these models, the flange sheets (plates) and stiffeners were presumed to have no primary imperfection.

For modelization of the cracks due to the web-flange welding, with regards to the previous studies, the idea of separating flange and web elements of the plate girders in required lengths was used. For modelization of the area of web-flange weld plates with one centimeter width and with the same thickness as the web plate were used.

Since metal plates are used in plate girders, the shell element group is the best choice among various elements of software. Shell element group contains two types of elements: the Thin shell and the Thick shell. The former was used in the modelization of plate girders after studies carried out through the program guide and with regards to previous studies (Corcetti 2003, Nicola, 2000].

This type of element in turn contains four types of 3,4,6 and 8 node elements, of which only the 8-node element, known as QLS8, is capable of geometric nonlinear analysis and as appropriate for clearer and more precise illustration of local buckling deformations and explanation of the effects of plasticity.

Therefore, for modelization this type of element was used in squares with $5_{cm}$ sides, so that in this 8-node element, 4 nodes were in corners of the square and the other 4 were in the middle of the sides. Degrees of freedom of this element shows in the figure 3.

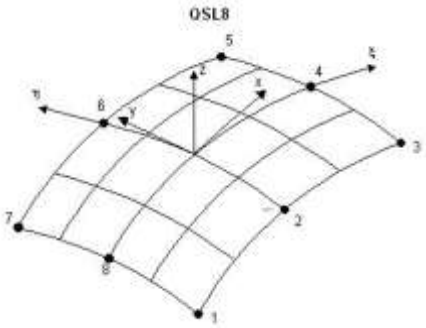


**Figure 3: Degrees of freedom of QSL8 in LUSAS software.**

The QSL8 element is capable of analyzing plastic and is, therefore the most appropriate element for modelization. Its speed of analysis is low due to its 8 nodes, whereas its computation accuracy is high.
Because of plastic deformations, nonlinear analysis of materials was used in this study. For the definition of structural steel. The study used Isotropic materials and Mild steel with Poisson`s ratio of 0.3 and modulus elasticity of $2.1\times10^{6} kg/cm^{2}$. The behavior of materials was assumed to be 4 line elastic-plastic (figure 4).

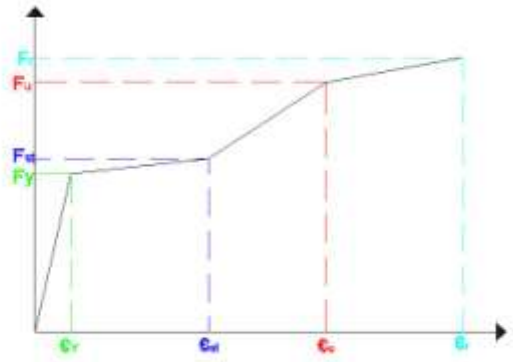


**Figure 4: The stress-strain graph of selected materials**

For selected materials, specifications of St40kis steel was considered. The values of stress and strain of this type of steel in yielding and rupture states is depicted in table 1.

**Table 1: Stress-strain values of st40kis steel**

| | Strain | Stress (Mega Pascal) |
|---|---|---|
| Yielding stress ( $F_y$ ) | 0.001313 | 275.8 |
| Strain hardening stress ( $F_{st}$ ) | 0.01059 | 285.073 |
| Ultimate stress ( $F_u$ ) | 0.05786 | 448.175 |
| Rupture stress ( $F_r$ ) | 0.09233 | 482.65 |

Since the Von Mises criterion is very appropriate for the analysis of models with ductile materials of less volume strain and it facilitates the use of large steps of load increase along with faster convergence (Nicola, 2000), this criteria based on deflective e energy of material is used in this study.
As depicted in figure 2, a uniform linear distributed load executed on upper flange is used for modelization of samples and for nonlinear analysis the load is increased steadily.
In end panels of the girder, using the definition of 2 types of fixed and mobile hinged supports we modeled plate girders with uniform distributed load.

It should be mentioned that in all these models, in order to prevent the torsional buckling of flanges. They were braced at the impact site of stiffeners, both in the compressive and tension regions, using lateral supports along the girder.

The two aspects of Nonlinear analysis are: nonlinear material analysis and nonlinear geometric analysis. The latter is considered when equation formation according to the non-deformed state of the structure is not suitable. For the purpose of nonlinear analysis, the amount of load increase should be determined in every stage of loading. This amount will be added step by step to the previous amounts of the load. This gradual increase with the definition of primary limits and the amount of increase at every stage will be done automatically bye the software. In the linear analysis of limited elements, because of the indefinite form of the distorted structure, a lagrange coordinate system is selected to determine the nonlinear equations of the limited element which is based on the previous equations. There are often two types of lagrange comparative coordinate system:

1. Total lagrangian coordinates
2. Update lagrangian coordinates

In total lagrangian coordinates, all equations in their present distorted state are determined according to the equations of the primary form of the structure. But in update lagrangian coordinates equations in their present distorted state are based on equations related to the distorted form of the previous state.

In this study, total lagrangian coordinates are used for nonlinear calculations. Also, for transition of fixed load analysis by arc length method, we used current stiffness parameter value with presupposition value of 0.4. After establishing these parameters for nonlinear calculations, models were analyzed.

Since fine 8-node squares were used in these models, the time for analysis of each and every model was very long, taking from 28 to 33 hours.

***Introduction of Samples***

In this paper, some variables were considered in surveying the impact of the crack of the flange to web weld of the plate girders. These variables are as follows:

1. Length of the crack:

Given that cracks were formed and distributed by different factors and then controlled, $10_{cm}$ and $30_{cm}$ cracks were made in the site of the flange to web weld of the plate girder.

2. Location of the crack:

Cracks were formed in 4 different locations in the compressive flange to web weld of the plate girder in the second panel (on the support) and 3rd, 5th and 8thpanels (in the middle of the girder). It should be mentioned that panel numbering starts from the support of the left side of the modeled girder in the software. Also, in order to compare the impact of cracks in the tensile flange to web weld with that of cracks formed in the compressive flange to web weld, cracks in different lengths were made in the tensile flange - web weld in the 3rd panel of the plate girder and then studied.

3. Slenderness Ratio of plate girder ( $h/t_w$ ):

In this study, plate girders with 125 and 250 slenderness ratios were used. To alter the slenderness ratio of plate girders, we changed the thickness of their web, so that in models with a slenderness ratio of 125, the web thickness was 8 mm and in those with a slenderness ratio of 250, it was 4mm.

For the labeling of samples with cracks in their flange to web weld the general form of G_a(t or b)n was used, in which (G), represents slenderness ratio, (a) stands for the length of the crack and (n) indicates the number of the panel where the crack has occurred. If the crack occurred in the tensile web-flange weld, the letter (b) would be used and if it occurred in the compressive web-flange weld, the letter used would be (t).

For the labeling of the crack samples, the form G-without crack was used. For example, a sample labeled 125_30t5 is indicative of a plate girder with slenderness ratio of 125 and a $30_{cm}$ crack which occurred in compressive web-flange weld on the 5th panel.

***Impact of Cracks in Flexural Behaviour of Plate Girders***

After modelization and analysis of samples, the results are compared by drawing load-lateral displacement and load-vertical displacement graphs. Figures 5 and 6 illustrate the load-lateral

displacement graphs for plate girders with slenderness ratio of 125 and cracks of $10_{cm}$ and $30_{cm}$ in the web-flange weld.

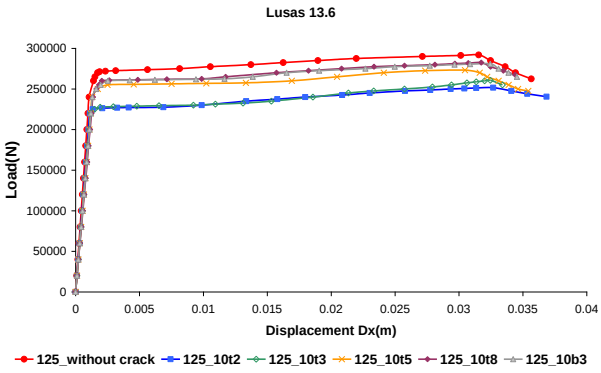


**Figure5: graph showing load-lateral displacement for girders with $10_{cm}$ cracks**

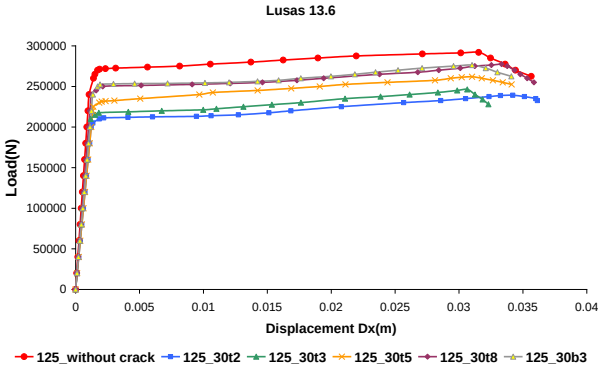


**Figure 6: graph showing load-lateral displacement for girders with $30_{cm}$ cracks**

In figure 7 and 8, the graphs of load-vertical displacement for the same models, with regards to the absolute value of the vertical displacement (considering the negative direction of the vertical deflection in the coordinates used for modelization) have been drawn.

These graphs are used to calculate the maximum bending moment tolerable for the samples by finding their maximum ultimate load.

These figures show that the bending capacity of the girder has direct relation to the length of the crack, so that for example a $10_{cm}$ crack in the compressive web-flange weld of a plate girder with slenderness ratio of 125 on the $2^{nd}$ panel reduces its ultimate bending capacity by %13.8, whereas a $30_{cm}$ cracks on the same girder and in the same location produces an %18 reduction in its bending ultimate capacity.

The study of load-vertical displacement graphs (figure 7 and 8) indicate that they start primarily in a linear manner with a rather sharp rise, but in the nonlinear stage the rise increases drastically with a little increase in the amount of force.

With regards to these graphs, it can be concluded that if cracks were made in the tensile web-flange weld, the effect on the reduction of the bending capacity of the plate girder would be very little (i.e. the %3.74 reduction in the ultimate bending resistance due to $10_{cm}$ crack on the tensile web-flange weld on the $3^{rd}$ panel), whereas if the same crack with equal length occurred on the compressive web-flange weld of the same panel, the ultimate bending resistance would be reduced by % 10.7.

Figure 7: load-vertical displacement graph for plate girders with $10_{cm}$ cracks.

Figure 8: load-vertical displacement graph for plate girders with $30_{cm}$ cracks.

In figure 9, the bending ultimate moment graph of samples has been drawn with regards to the location of the cracks (according to the number of the panel with crack from the left edge of the girder). The dotted horizontal line indicates crackles samples. The confluence of this line and the vertical coordinate

represents the bending ultimate moment, tolerable for these models. The expression "top crack" has been applied to cracks of the compressive web-flange weld and 'bottom crack' to cracks of the tensile web-flange weld.

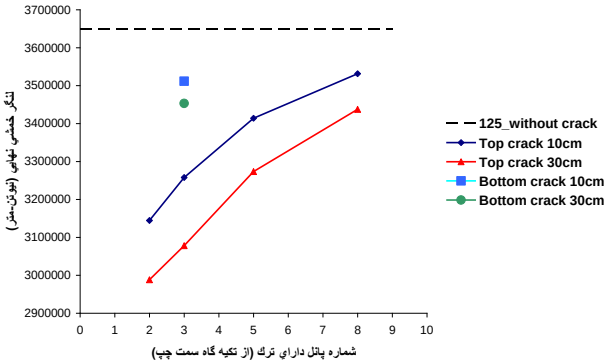


**Figure 9: The bending ultimate moment graph and the location of crack in plate girders with slenderness ratio of 125**

According to figure 9, it can be said that the most critical state for all the three forms of $10_{cm}$ and $30_{cm}$ cracks is when they occur in the $2^{nd}$ panel (near the support). The more inclined the location of the crack toward the middle girder, the fewer the change in the bending ultimate moment in comparison with the crackles sample. This graph also demonstrates clearly that in plate girders with 125-slenderness ratio, the length of the crack plays an important role in the reduction of its bending ultimate capacity and with the increase of the length of the crack its impact in the reduction of the ultimate strength increases.

According to this graph, a $10_{cm}$ crack in the web-flange weld of the plate girder near the support can reduce the ultimate bending moment by 503849 Newton-meter whereas a $10_{cm}$ crack in the $5^{th}$ panel of the same type of plate girder causes a reduction of 374695 Newton-meter in the ultimate bending moment of the plate girder. Therefore, it can be concluded that the variable of location of the crack is more effective in the reduction of the ultimate bending capacity than the variable of length of the crack in the web-flange weld of a plate girder.

Since in every crack length only one model for the crack occurring in the tensile web-flange weld of the plate girder has been analyzed, the result of these graphs have been demonstrated with a dot in figure 9. Moreover, as is shown in figure 9, the impact of cracks in the tensile web-flange weld isles compared to that in the compressive web-flange weld, in that, if the crack in the tensile web-flange weld occurred with 125 slenderness ratio, the girder can tolerate a higher bending moment.

Figure 10 and 11 depict the load-lateral displacement graph for plate girders with 250 slenderness ratio. According to LRFD code, these types of plate girders are considered as plate girders with slender web.

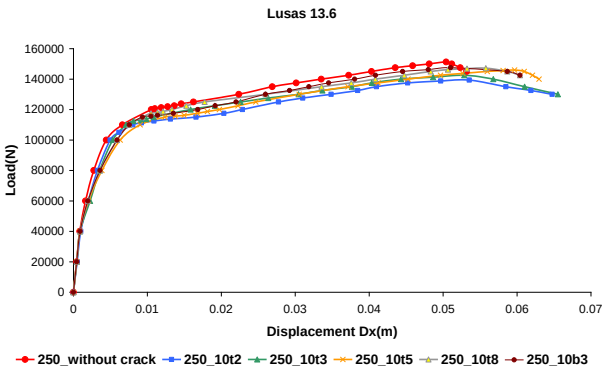


**Figure 10: Load-lateral displacement graph for plate girders with $10_{cm}$ cracks**

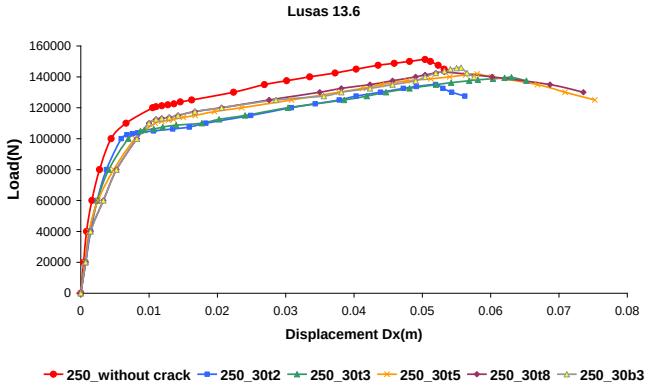


**Figure 11: Load-lateral displacement graph for plate girders with $30_{cm}$ cracks**

As is demonstrated in figures 10 and 11, plate girders with 250 slenderness ratio also experience an increased deflection of the ultimate bending capacity with the increase of the length of the crack. Moreover, as the distance between the crack location and the support increases, the strength-reduction factor is reduced.

The comparison of figures 10 and 11 with figures 5 and 6 indicates that in nonslender plate girders (with 125 slenderness ratio) the buckling and post-buckling loads differ slightly. Thus, the post-buckling capacity plays an inconsiderable role in providing plate girder strength. Whereas in slender plate girders (with 250 slenderness ratio) the buckling load accounts for the greaten part of plate girder strength.

In the other words, in plate girders with 125 slenderness ratio (nonslender) because of the increase in the ratio of cross section area of web to flange, it is not possible to use the post-buckling capacity of the plate girder fully. Therefore, it can be concluded that with the reduction in the ratio of the cross section area of the web to the flange, the cross section of the plate girder will be more economical.

Figures 10 and 11 illustrate that the load-lateral displacement graph was linear before reaching the buckling load, and that it become multi linear after the increase of the load, which is related to post-buckling capacity. Also, with a slight increase in the load, a considerable displacement occurs just after the post-buckling load.

In the figure 12 and 13. The load-vertical displacement graphs show plate girders with 250 slenderness ratio.

These graphs are linear at the beginning, but with the increase of the load, the difference in displacement occurs with a steady fall and it is limited.

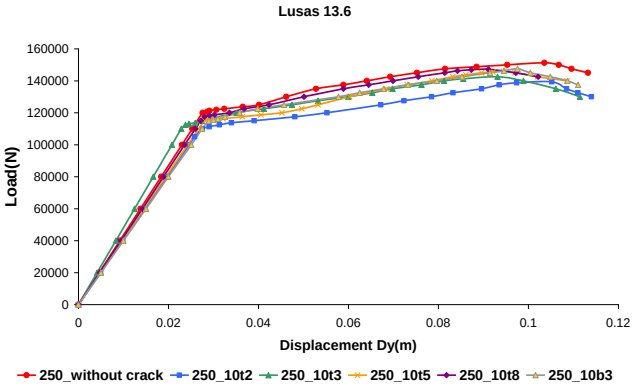


**Figure 12: Load-vertical displacement graph for plate girders with $10_{cm}$ cracks**

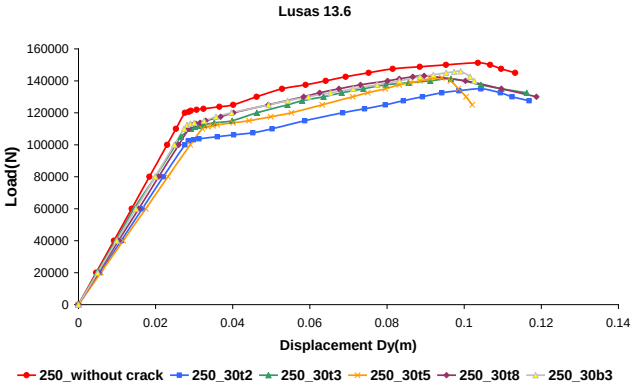


**Figure 13: Load-vertical displacement graph for plate girders with $30_{cm}$ cracks**

In these graphs, as in graphs of samples with 125 slenderness ratio, we can see that once the load reaches the yielding limit, the vertical displacement of samples increases considerably with a slight increase of the imposed load.

According to these graphs and the ultimate loads tolerable for these samples, the maximum reduction in the ultimate bending capacity occurs in samples with cracks of $30_{cm}$ length in the compressive web-flange weld in the second panel of the plate girder and this crack cause a %10.74 reduction in the ultimate bending strength of the plate girder. Additionally, the graphs show that the impact of the presence of a crack in the tensile web-flange weld is less than that of a crack in the compressive web-flange weld of a plate girder.

The graph in figure 14 shows the ultimate bending capacity of the plate girder with 250 slenderness ratio in relation to the location of the crack occurring in the web-flange weld. With regards to this graph, it can be concluded that the nearer the reduction of the bending strength will be. Moreover, with the increase in the length of the crack, its impact on the reduction of the ultimate bending strength will increase. Thus, the graph relating to the $30_{cm}$ crack is placed below the graph relating to the $10_{cm}$ crack.

In this graph, as in graph of figure 9, the reduction of the ultimate bending capacity is lower when the crack is in the tensile web-flange weld rather than in the compressive web-flange weld.

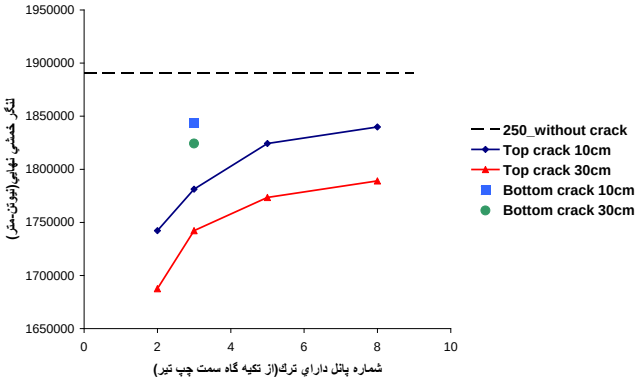


**Figure 14: The graph of the ultimate bending capacity and the location of the crack in plate girders with 250 slenderness ratio**

As it is seen, the comparison of figure 9 and 14 shows that the increase in slenderness ratio results in the decrease in the inclination of the lines connecting the points for different lengths of crack. This indicates that, in plate girders with higher slenderness ratio, the difference in the reduction rate of the ultimate bending moment decreases when cracks occur in different panels.

Figure 15 depicts the lateral pitch contour relating to the first stage of loading where the imposed load is equal to 20000 Newton/meter. According to this figure, all panels have similar deformations at the primary stages of loading. It should be mentioned that, due to the symmetry on the two sides of the span from its center point, in all the figures of this section, for better magnification, only half of the girder span has been studied.

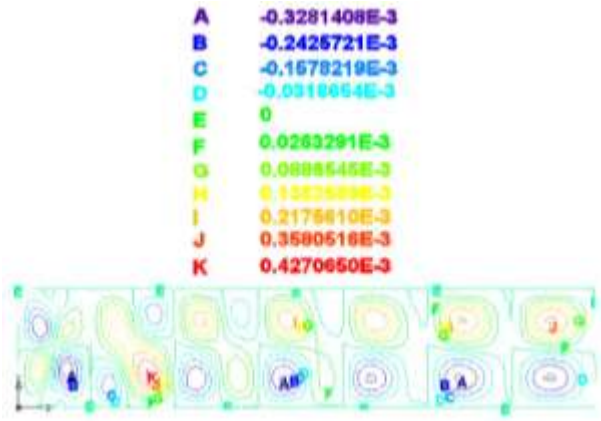


**Figure 15: lateral pitch contour of plate girders with 250 slenderness ratio with no cracks and under the impact of a 20000 Newton/meter load**

Figure 16 depicts the lateral pitch contour for model 250-30t3 under a load of 20000 Newton/meter. The comparison of figure 15 and 16 shows that in the primary stage of loading in the model with a crack, the location of maximum lateral pitch would be at the place where the crack has occurred, whereas in the crackles model, the maximum lateral pitch would occur in the lower region of the 2nd panel, next to the support.

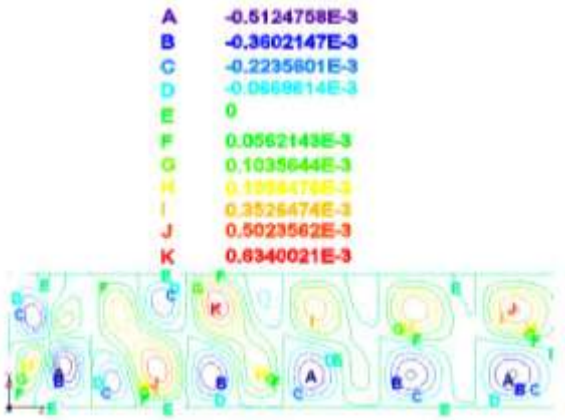


**Figure 16: lateral pitch contour of plate girder with 250 slenderness ratio in model 250_30t3 under influence of a 20000 newton/meter load**

***Assessment of the Results According to the Code of AISE-LRFD:***

In this section, considering the geometric features of the models shown in figure 2, buckling and post-buckling load of crackles plate girders are calculated according to the LRFD code and are compared with the results obtained from the analysis of the studied models using finite element tools of LUSAS software. To compare the effect of cracks on the theoretical relations of the plate girders, the results of

these relations ore studied in conjunction with the results of the analysis of models with $30_{cm}$ cracks (the most critical length of cracks in this study) in various locations.

First, the buckling and post-buckling capacities of plate girders with 250 slenderness ratio are calculated according to the theoretical relations of the LRFD code.

$$k = 5 + \frac{5}{(\frac{a}{h})^2} = 14.38$$

$$1550\sqrt{\frac{k}{F_y}} = 1550\sqrt{\frac{14.38}{2750}} = 112$$

$$1940\sqrt{\frac{h}{F_y}} = 1940\sqrt{\frac{14.38}{2750}} = 140 \Rightarrow 250 \succ 140$$

$$C_v = \frac{3033800 \times k}{(\frac{h}{t_w})^2 \times F_{yw}} = \frac{3033800 \times 14.38}{(250^2) \times 2750} = 0.2538$$

If $\frac{h}{t_w} \succ 1550\sqrt{\frac{K}{F_{y_W}}}$, then the relation (2) will be true.

$$V_n = 0.6 \times A_w \times F_{y_W} \times \left[ C_v + \frac{1 - C_v}{1.15 \times \sqrt{1 + \left(\frac{a}{h}\right)^2}} \right] \quad (2)$$

In relation (2) the first part, indicates the shearing buckling strength and the second part, the shearing post-buckling strength. Therefore, the buckling capacity will be:

$$V_n = 0.6 \times 100 \times 0.4 \times 2750 \times 0.2538 = 16750.8kg$$

$$q = \frac{V_n \times 2}{L} = \frac{16750 \times 2}{10} = 3350\frac{kg}{m} \Rightarrow q = 32863.5\frac{N}{m}$$

And the post-buckling capacity will be:

$$V_n = 0.6 \times 100 \times 0.4 \times 2750 \times \left[ \frac{1 - 0.2538}{1.15 \times \sqrt{1 + (0.73)^2}} \right]$$

$$V_n = 34589.5kg$$

With regards to the amounts obtained for the calculated buckling and post-buckling capacities, the ultimate post-buckling load resulting from the theoretical relations will be as follows:

$$67864.6 + 32863 = 100727.6\,{}^{N}\!/_{m}$$

Considering the results of the analysis of models as well as the results of the buckling and post-buckling loads obtained from the theoretical relations in the LRFD code for plate girders with 250 slenderness ratio, it is seen that cracks with different lengths and locations have little impact (influence) on the buckling and post-buckling loads of these plate girder and that they only reduce their ultimate tolerable load. Additionally, it is noted that the results of the analysis of models are appropriately compatible with the results of the theoretical relations of the LRFD code. The buckling load lies in the linear part, while the post-buckling load is in the multi-linear section of the load-lateral displacement graphs of the models.

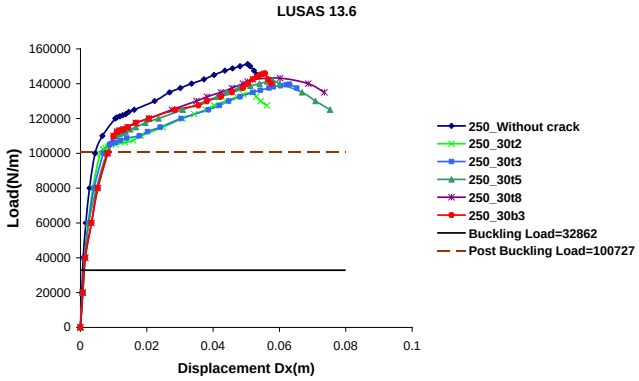


**Figure 17: load-lateral displacement graph showing bucking and post-buckling capacities for models with 250 slenderness ratio**

The results show that, in plate girders with 250 slenderness ratio, the buckling load comprises %21.73 of the ultimate load, while the post-buckling load includes %66.59 of it.
Next, the buckling and post-buckling capacities of the plate girders with 125 slenderness ratio will be calculated:

$$k = 5 + \frac{5}{(\frac{a}{h})^2} = 14.38$$

$$1550\sqrt{\frac{k}{F_y}} = 1550\sqrt{\frac{14.38}{2750}} = 112$$

$$1940\sqrt{\frac{h}{Fy}} = 1940\sqrt{\frac{14.38}{2750}} = 140 \Rightarrow 112 \prec 125 \prec 140$$

$$\Rightarrow C_V = \frac{1550\sqrt{(\frac{14.38}{2750})}}{\frac{h}{t_w}} = \frac{1550 \times 0.0723}{125} = 0.896$$

Because relation (2) is also true for this type of plate girder, therefore the buckling capacity will be as follows:

$$V_n = 0.6 \times 100 \times 0.8 \times 2750 \times 0.896 = 118272kg$$

$$q = \frac{V_n \times 2}{L} = \frac{118272 \times 2}{10} = 23654.4\frac{kg}{m} \Rightarrow q = 232049\frac{N}{m}$$

While the post-buckling capacity will be:

$$V_n = 0.6 \times A_w \times F_{y_W} \times \left[\frac{1 - C_v}{1.15 \times \sqrt{1 + \left(\frac{a}{h}\right)^2}}\right]$$

$$V_n = 0.6 \times 100 \times 0.8 \times 2750 \times \left[\frac{1 - 0.896}{1.15 \times \sqrt{1 + (0.73)^2}}\right]$$

$$V_n = 9641.6kg$$

$$q = \frac{2 \times V_n}{L} = \frac{19283}{10} = 1928.3 \frac{kg}{m} = 18916.6 \frac{N}{m}$$

Hence the ultimate post-buckling load is as follows:

$$232049 + 18916 = 250965 \, N/m$$

As is seen in figure 18, because of the occurrence of $30_{cm}$ cracks in critical panels ($2^{nd}$ and $3^{rd}$) in the compressive web-flange weld of the plate girder, the buckling and post buckling capacities of the models have been reduced and even the ultimate tolerable load for them is less than the post-buckling capacity obtained from theoretical relations for the crackles plate girders. Additionally, the occurrence of $30_{cm}$ cracks in the $5^{th}$ panel in the compressive web-flange weld of a plate girder causes the reduction of its post-buckling capacity in comparison to the capacity obtained in theoretical relation for crackles models.
In plate girder of this type, the buckling load comprises %79.5 of the ultimate load and the post-buckling load includes %86 of it.

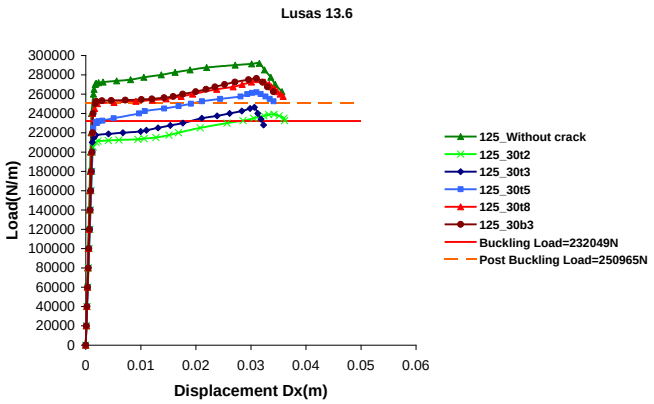


**Figure 18: Load-lateral displacement graph showing buckling and post-buckling capacities for models with 125 slenderness ratio**

## CONCLUSION

Because of the possibility of occurrence of cracks in welded connection for various physical and environmental reasons, and in order to study the influence of possible cracks in the web-flange weld of the plate girders, a number of models with and without cracks were built using the finite element of LUSAS software and were investigated through nonlinear geometric and material analysis. The effect of the geometric imperfection in this analysis and the following results were obtained:

1- In this study, the highest reduction rate of bending capacity (%18) was seen in plate girders of 125-30t2 models where cracks had occurred in the $2^{nd}$ panel (in near the support). This indicates that the crack of the web-flange weld will have a greater destructive effect if it occurs in region near the support. The nearer the location of the crack is to the center of the girder, the lower the ultimate bending strength-reduction factor will be.

2- The reduction of the ultimate bending capacity of the plate girder under the influence of cracks in the web-flange weld is in direct relation to the length of the crack.

3- With the increase in the slenderness ratio of the plate girder (the web area to flange area ratio), the effect of cracks on the finite bending capacity reduction increase.

4- The results show that the crack-location variable is more significant and effective than the crack-length variable. For instance a $10_{cm}$ crack in the $2^{nd}$ panel (in near the support) of a plate girder with 250 slenderness ratio causes a reduction of %7.85 in the ultimate bending capacity, whereas a $30_{cm}$ crack in the $5^{th}$ panel of the same plate girder reduces the ultimate bending capacity by %6.19.

5- The presence of cracks in the compressive web-flange weld is more significance and critical than the occurrence of cracks in the tensile web-flange weld of a plate girder.

6- The comparison of the results of the analysis of different models with without cracks using the tools of LUSAS software and the results obtained from theoretical relations of the LRFD code, revealed that in slender plate girders with lower slenderness ratio, the occurrence of cracks in critical panels and near the support causes the reduction of buckling (and sometimes post-buckling) capacity of the plate girders compared to the crackles ones. In contrast, in slender plate girders with higher slenderness ratio, the presence of cracks does not affect their buckling or post-buckling capacity, but reduces their ultimate tolerable load.

7- A study of the load-vertical displacement graphs show that the gradient in the linear section of the graphs of models with cracks differs from that of crackles ones, whereas the load-lateral deflection graphs of most models do not show a great difference in the linear section. However, the difference exists only in the multi-linear sections relating to the post-buckling capacity of plate girders, which indicates that comparison and monitoring of the load-vertical defection graphs are more effective in the detection of cracks.

## REFERENCES

**Akbari H (2006).** The Impact of Cracks of the Stiffener - WebWeld of the Plate Girders on their Buckling and Post-buckling Capacity. Master's Degree Thesis, Civil Engineering-Structures, The Islamic Azad University of Maragheh.

**Corcetti R (2003).** Web breathing of full-scale slender I-girders subjected to combine action of bending and shear. *Journal of Constructional Steel Research* **59**(3) 271-290.

**Farhoody Mohammad Zadeh F (2007).** A Study of the Impact of Cracks of the Flange-Web Weld of Plate Girders on their Flexural Ultimate Buckling Capacity. Master's Degree Thesis, Civil Engineering-Structures, The Islamic Azad University of Maragheh.

**Joemkee Paik, Satish Kumar YV and Jae Myung Lee (2005)**. Ultimate Strength of cracked plate elements under axial compression or tension. *Thin-Walled Structures* **43**(2) 237-272.

**Nicola G (2000).** Cross-Sectional Compactness and Bracing requirements for Hybrid HPS Girders. Master's thesis, University of Pittsburgh.

**Okura I, Yen BT and Fisher JE (1993).** Fatigue of Thin walled plate girders. *Structural Engineering International* **3**(1) 39-44.

**Roberts TM and Davies AW (2002).** Fatigue induced by plate breathing. *Journal of Constructional Steel Research* **58**(12) 1495–1508.

**Tahooni Shapour (2001).** *Designing Steel Structures* (Elm &Adab Publishings) 4th edition.